



1 **Basin-scale multi-objective simulation-optimization modeling for**  
2 **conjunctive use of surface water and groundwater in northwest China**

3 Jian Song<sup>a</sup>, Yun Yang<sup>b</sup>, Xiaomin Sun<sup>c</sup>, Jin Lin<sup>c</sup>, Ming Wu<sup>d</sup>, Jianfeng Wu<sup>a,\*</sup>, Jichun Wu<sup>a</sup>

4

5 <sup>a</sup> Key Laboratory of Surficial Geochemistry, Ministry of Education; Department of  
6 Hydrosociences, School of Earth Sciences and Engineering, Nanjing University, Nanjing,  
7 210023, China

8 <sup>b</sup> School of Earth Sciences and Engineering, Hohai University, Nanjing, 210098, China

9 <sup>c</sup> Nanjing Hydraulic Research Institute, National Key Laboratory of Water Resources and  
10 Hydraulic Engineering, Nanjing, 210029, China

11 <sup>d</sup> Institute of Groundwater and Earth Sciences, Jinan University, Guangzhou, 510632, China

12

13

14

15

16 \*Corresponding author: Jianfeng Wu ([jfwu@nju.edu.cn](mailto:jfwu@nju.edu.cn); [jfwu.nju@gmail.com](mailto:jfwu.nju@gmail.com))

17

18



19 **ABSTRACT**

20 In the arid inland basin of China, the long-term unregulated agriculture irrigation from  
21 surface water diversion and groundwater abstraction has caused unsustainability of water  
22 resources and degradation of ecosystems. This requires integrated management and  
23 conjunctive use of surface water (SW) and groundwater (GW) at basin scale to achieve  
24 scientific decision supports for water resources allocation in China. This study developed a  
25 novel multi-objective simulation-optimization (S-O) framework for sustainably conjunctive  
26 use of SW and GW in Yanqi Basin (YB), a typical arid region with intensive agricultural  
27 irrigation in northwest China. The S-O model integrates the new epsilon multi-objective  
28 memetic algorithm ( $\epsilon$ -MOMA) with the MODFLOW-NWT based simulation model for  
29 examining the hydraulic interactions between SW and GW. Four conjunctive management  
30 objectives, involving maximizations of total water supply rate, groundwater storage change and  
31 surface runoff inflow to Bosten Lake, and minimization of total water delivery cost, were  
32 considered to explore the tradeoffs between socioeconomic development and environmental  
33 demands. The combined multi-objective SW and GW management model can achieve the  
34 tradeoffs in high-order objective spaces by considering groundwater abstraction in the  
35 irrigation districts and surface water diversion from the river, so as to avoid the prevalence of  
36 decision bias caused by the low-dimensional optimization formulation. Decision-makers are  
37 then able to identify their desired water use schemes with preferred objectives in the  
38 post-optimization and achieve maximal socioeconomic and ecological benefits. Furthermore,  
39 three representative runoff scenarios under changing climatic conditions were specified to  
40 quantify the influence of decreasing runoff in Kaidu River on the YB water management.  
41 Results show that runoff reduction would be of great negative impact on the total water supply,  
42 surface runoff inflow to the lake and regional groundwater storage in the aquifer. Therefore, the  
43 integrated SW and GW management is of critical importance for the protection of the fragile



44 hydro-ecosystem under changing climatic conditions.

45 **Keywords:** Multi-objective optimization; water resources management; conjunctive use; Yanqi  
46 Basin; Bosten Lake

## 47 1. Introduction

48 In arid and semi-arid inland basin, the intensive irrigation for agricultural development  
49 caused the deterioration of natural ecosystem sustained with scarce water resources (Wichelns  
50 and Oster, 2006; Wu et al., 2016). In general, the irrigation water is diverted from groundwater  
51 (GW) abstraction and surface water (SW) diversion in the densely populated oasis regions in  
52 northwest China (Liu et al., 2010; Wu et al., 2014). Therefore, the conjunctive management of  
53 GW and SW is essential for the requirement of local economic development and  
54 eco-environmental conservation (Khare et al., 2006; Safavi and Esmikhani, 2013; Singh, 2014;  
55 Hassanzadeh, et al., 2014; Wu et al., 2016). Yanqi Basin (YB) is a typical oasis in an arid  
56 inland basin located to the southern Tianshan Mountains in Xinjiang Province, northwest China.  
57 The surface water resource in YB is mainly composed of a river and a lake, namely Kaidu  
58 River and Bosten Lake, the biggest freshwater inland lake in China (Wang et al., 2014; Zhou et  
59 al., 2015). Kaidu River supplies approximately 95% of total inflow to Bosten Lake (Gao and  
60 Yao, 2005; Liu et al., 2013; Yao et al., 2018) which is the major water source of the Kongqi  
61 River recharged by an artificial pumping station built in 1983. Therefore, the water supply  
62 scheme in YB dominates the water balance in Bosten Lake and has a significant influence on  
63 the Kongqi River and the lower reaches of Tarim River where the serious water crisis has taken  
64 place. With the intensive agricultural development, surface water diverted from Kaidu River  
65 can no longer meet crop water requirements. Thus, groundwater became the alternative water  
66 source for crop production whereas the excessive groundwater exploitation has caused the  
67 deterioration of local ecosystem associated with the decline of groundwater level and altered  
68 the hydraulic interaction between GW and SW (Hu et al., 2007; Zhang et al., 2014; Tian, et al.,



69 2015, Yao et al., 2015). For this reason, the integrated SW and GW management is essential for  
70 rational utilization of water resources in the arid inland basin due to the physical water scarcity.

71 In the water resources planning and management, the simulation-optimization (S-O)  
72 methods can provide optimal schemes to guide and inform stakeholders (Maier et al., 2014).  
73 Evolutionary algorithms have been integrated with simulation model to tackle intricate SW and  
74 GW management model due to the effectiveness of solving non-linear and multimodal  
75 optimization problems (McPhee and Yeh, 2004; Yang, et al., 2009; Safavi and Esmikhani, 2013;  
76 Singh and Panda, 2013; Rothman and Mays, 2013; Wu et al., 2014; Parsapour-Moghaddam et  
77 al., 2015; Wu et al., 2016). Yang et al. (2009) considered conflicting bi-objectives with the  
78 conjunctive use of GW and SW to achieve optimal pumping and recharge schemes. Rothman  
79 and Mays (2013) developed an optimization model including cost control, aquifer protection  
80 and growth objectives using multi-objective genetic algorithm. Wu et al. (2016) performed the  
81 temporal optimization of monthly volume of surface water diverted from Heihe River by  
82 linking a physical-based integrated modeling with a simple single-objective management  
83 model. However, these studies rarely consider many-objective optimization in the basin-scale  
84 water management with conjunctive use of SW and GW. The management model including the  
85 typical single objective or bi-objective formulation probably results in the decision bias (*i.e.*,  
86 cognitive myopia or short-sightedness) due to the sub-optimal solution only considering the  
87 fewer preference criteria (Kasprzyk et al., 2012, 2015; Woodruff et al., 2013; Matteo et al.,  
88 2019). Therefore, for water management with the strong interactions between SW and GW in  
89 the basin-scale water cycle, the optimal water use practice calls for decision-maker to consider  
90 multiple conflicting management objectives. In general, the management objectives are  
91 composed of maximizing water use demands (*e.g.*, total volume of surface water and  
92 groundwater use), minimizing the capital and operation costs of water delivery and minimizing  
93 the effect of water resources exploitation on the hydro-ecosystem to ensure sufficient



94 environmental flow (*e.g.*, the regional groundwater storage and surface runoff inflow to the  
95 terminal lake).

96 Multi-objective evolutionary algorithms (MOEAs) can obtain the tradeoff solutions that  
97 cater to multiple competing objectives and reflect comprehensive decision information for  
98 practitioners in real-world applications (Beh et al., 2017; Eker and Kwakkel, 2018). However,  
99 many-objective optimization often suffers from the domination resistance phenomenon  
100 (Purshouse and Fleming, 2007; Hadka and Reed, 2013), which shows that the diminishing  
101 Pareto-sorting capacity triggers many non-dominated solutions in the population and then  
102 results in stagnation of evolutionary search. Hadka and Reed (2013) developed a novel Brog  
103 MOEA, which employed auto-adaptive six recombination operators,  $\epsilon$ -box technique for the  
104 Pareto sorting and injection strategy to avoid stagnation of evolutionary search and archived  
105 optimal solutions in addressing many-objective optimization. In order to enhance the local  
106 optimality of solutions, a memetic algorithm composed of the biological process of natural  
107 selection and cultural evolution capable of local refinement was applied to ensure the  
108 convergence of the MOEA (Sindhya et al., 2011; 2013). This study attempts to utilize the  
109  $\epsilon$ -dominance concept, the modified auto-adaptive recombination operators to alleviate  
110 domination resistance problem, and a local search operator to enhance the local optimality of  
111 archived solutions with the framework of NSGA-II (Deb et al., 2002). The improved algorithm,  
112 named epsilon multi-objective memetic algorithm ( $\epsilon$ -MOMA), is applied to the many-objective  
113 optimization of conjunctive management of SW and GW for agricultural irrigation in YB.

114 In this study, a regional numerical model using MODFLOW-NWT (Niswonger, 2011) is  
115 developed for quantitatively evaluating water budget and interaction of river-lake-groundwater  
116 in YB. The model is calibrated according to long-term series of observation data during  
117 simulation period from 2003 to 2013. Kaidu River and Bosten Lake are simulated with  
118 Streamflow-Routing package (SFR2) (Richard and David, 2010) and Lake package (LAK3)



119 (Michael and Leonard, 2000). The lake and river simulation is calibrated based on observed  
120 lake level and runoff data at the gaging stations, respectively. Then, a well-calibrated model is  
121 linked with the novel  $\varepsilon$ -MOMA to explore optimal water supply schemes which consider  
122 multi-stakeholders' benefits simultaneously. Moreover, in order to encourage decision-makers  
123 to use the optimized schemes, an interactive tool is employed to visualize and analyze all the  
124 Pareto-optimal solutions and provide suggestions on the practical operation of water allocation.  
125 Kaidu River mainly gains water from seasonal precipitation that runs off the mountainous  
126 landscape and snow and glacier that melts in the upper Tianshan Mountains region known as a  
127 main water tower in the Central Asia. Dashankou gauging station is the dividing point between  
128 midstream and downstream of Kaidu River and the inlet of the basin where most of the river  
129 runoff flows into YB. Therefore, the runoff variation in Dashankou station, which is highly  
130 sensitive to the changes of precipitation and glacier mass loss dominated by the climate change,  
131 greatly affects the water resources and water cycle in Kaidu River watershed. Three  
132 representative runoff scenarios under the future climatic conditions are then specified to  
133 explore the effects of runoff reduction in Kaidu River on the integrated SW and GW  
134 management practices.

135 This study firstly constructs a multi-objective SW and GW management model to  
136 consider water supply and environmental benefits including regional groundwater storage and  
137 surface runoff inflow to lake. Then the spatial conjunctive optimization of surface water  
138 diversion and groundwater abstraction is implemented using the novel multi-objective  
139 evolutionary algorithm ( $\varepsilon$ -MOMA). The optimization results demonstrate that water managers  
140 can achieve the optimal schemes constrained by satisfying the water demands and sustaining  
141 the fragile hydro-ecosystem in YB. The implications from the optimization under the runoff  
142 reduction scenarios also provide valuable insights for water use practices in the face of climate  
143 changes in the arid inland basin.



## 144 **2. Methodology**

145 As shown in Fig. 1, this study aims to develop a multi-objective decision-making  
146 framework to optimize irrigation schemes of surface water diversion and groundwater  
147 abstraction for the integrated SW and GW management. The optimal schemes can assist  
148 decision-makers to achieve water demands and ensure water balance of hydro-ecosystem in  
149 YB. The optimization framework includes three main modules and their details are stated in  
150 the following sections.

### 151 **Figure 1.**

#### 152 *2.1 Problem formulation*

153 Module I in the optimization framework is to formulate an integrated SW and GW  
154 management model to implement water resources management in the basin. The water  
155 utilization patterns for irrigation are composed of diverting surface water from the inland reach  
156 of river basin and pumping groundwater from the regional aquifer. Therefore, the decision  
157 variables consist of the volume of surface water diversion in the aqueduct system and  
158 groundwater abstraction in the irrigation districts. In general, the optimal water supply  
159 strategies are maximizing the total volume of water supply and minimizing the capital and  
160 operation costs of water delivery. However, in the arid inland basin with water scarcity, the  
161 intensive agricultural development requires enough irrigation water to ensure local economic  
162 development while the sustainability of hydro-ecosystem also needs to follow specific  
163 requirements for maintaining environmental flows. For example, the excessive surface water  
164 diversion can significantly reduce the runoff inflow to the terminal lake, which causes obvious  
165 decline of lake level and results in the degradation of local hydro-ecosystem associated with  
166 the lake. Meanwhile, immoderate exploitation of groundwater stored in the aquifer to offset the  
167 surface water shortage triggers a series of environment problems (*e.g.*, dramatic decrease of



168 groundwater storage). Therefore, decision-makers should consider the total water supply rate  
169 and the cost of water delivery from multiple sources as socioeconomic metrics, and describe  
170 the runoff inflow to lake and groundwater storage as environmental metrics. Then, water  
171 managers can assess water use practices by weighing the four preference criteria. The  
172 performances of all schemes are evaluated based on the well-calibrated numerical model. The  
173 detailed formulation of management model can be seen in Section 3.3. Finally, the optimization  
174 model formulates water use practices as decision variables, socioeconomic and environmental  
175 metrics as management objectives, practical limitation of water exploitation and water  
176 demands for hydro-ecosystem as constrained conditions for the basin-scale SW and GW  
177 management.

## 178 *2.2 Optimization process*

179 Module II in the optimization framework illustrates the algorithmic process of  $\varepsilon$ -MOMA.  
180 The metaheuristic algorithms are superior to the classical optimization methods and have been  
181 successfully applied to water resources management and planning (Maier et al., 2014) due to  
182 the ability to solve complex problems with nonlinear, nonconvex and high-dimensionality  
183 features. To address domination resistance phenomenon in the many-objective optimization,  
184 the proposed algorithm integrates a  $\varepsilon$ -box technique, adaptive multi-operators recombination  
185 and a local search operator into the framework of NSGA-II. The key techniques can be  
186 recapitulated as follows.

187 The  $\varepsilon$ -box technique proposed by Laumanns et al. (2002) attempts to ensure convergence  
188 and diversity of Pareto-optimal solutions. Moreover, decision-makers can define the minimum  
189 resolution of objective vector with epsilon vector to satisfy their acceptable precision target and  
190 restrict the archive size. This study implemented the  $\varepsilon$ -dominance archive process after the fast  
191 non-dominated sorting of offspring individuals and alleviated the difficulties derived from the





192 domination resistance.

193 The auto-adaptive multi-operator recombination proposed by Hadka and Reed (2013) is a  
194 promising technique to select optimal operator for various optimization problems. The  
195 crossover probabilities of each operator are updated periodically based on the proportion of the  
196 solutions generated by each operator in the  $\varepsilon$ -dominance archive. The recombination strategy is  
197 essential for the complex many-objective and real-world optimization due to the inability to  
198 know a priori the optimal recombination operator. This study integrated the multiple  
199 recombination operators (*i.e.*, simulated binary crossover (SBX), differential evolution (DE),  
200 simplex crossover (SPX), parent-centric crossover (PCX), Laplace crossover (LX), uniform  
201 mutation (UM)) into the  $\varepsilon$ -MOMA to enhance search ability in higher order objective spaces.

202 The archived solutions are operated based on Gaussian perturbation in the neighborhood  
203 of the evolutionary individuals. Given an archived individual  $\mathbf{v}=(v_1, v_2, v_3, \dots, v_n)$ , the mutated  
204 individuals can be stated as:

$$205 \quad \mathbf{v}^+ = (v_1, v_2, \dots, v_i + p \times (m_i - w_i), \dots, v_n) \quad (1)$$

$$206 \quad \mathbf{v}^- = (v_1, v_2, \dots, v_i - p \times (m_i - w_i), \dots, v_n) \quad (2)$$

207 where  $\mathbf{v}=(v_1, v_2, \dots, v_n)$  is an  $n$ -dimensional decision variable vector;  $\mathbf{m}=(m_1, m_2, \dots, m_n)$  and  
208  $\mathbf{w}=(w_1, w_2, \dots, w_n)$  are two individuals randomly selected from the archive;  $c$  follows standard  
209 Gaussian distribution. The process is effective with the probability of  $1/n$  (Chen et al., 2015).  
210 The  $\varepsilon$ -MOMA revives the local search operator in every several generations. Therefore,  
211  $\varepsilon$ -MOMA possesses the ability of highly effective global search with adaptive recombination  
212 operator and epsilon domination to find higher quality and diverse solutions with local search  
213 operator in solving intricate many-objective optimization problem.

### 214 2.3 Visual analytics of Pareto-front

215 In the many-objective optimization, it is difficult for water managers to distinguish the



216 performance of single solution and discover desired schemes without the detailed visual  
217 analytics. Module III used an interactive visual analytics package, DiscoveryDV (Hadka et al.,  
218 2015; Kollat and Reed, 2007), to explore and analyze water management practices in the  
219 high-order objective spaces. The package employed multi-dimensional coordinate plot and  
220 parallel coordinate plot (Inselberg, 2009) to visualize Pareto-optimal solutions. Visualizing  
221 performance objectives can assist stakeholders to compare with the scheme before the  
222 optimization and select key tradeoff schemes with a clearer perspective (Matteo et al., 2019;  
223 Maier et al., 2014). Moreover, decision-makers can eliminate redundant schemes based on the  
224 preferred objectives or concerns and filter the optimal subsets those probably adopted by the  
225 experienced practitioners.

### 226 **3 Case study**

#### 227 *3.1 Study area*

228 YB is a typical oasis in an arid inland desert basin in the southern Tianshan Mountains,  
229 Xinjiang Province, northwest China and includes Yanqi County, Hejing County, Bohu County  
230 and Heshuo County, with a total area of about 7600 km<sup>2</sup> (Fig. 2). In the model domain, the  
231 northwest is mountainous and the south is a low-lying desert, and the terrain slopes from  
232 northwest to lower southeast. YB is located in the temperate zone of continental desert climate  
233 with an annual mean temperature of 14.6 °C, an annual precipitation of 50.7-79.9 mm, and a  
234 potential evaporation of 2000.5-2449.7 mm (Mamat et al., 2014). The basin is mainly  
235 composed of the Kaidu River, Huangshuigou River and Qingshui River. Kaidu River originates  
236 from the Hargat Valley and the Jacsta Valley in the middle part of the Tianshan Mountain with  
237 a maximum altitude of 5000 m and ends in Bosten Lake (Xu et al., 2016). Kaidu River is the  
238 largest inland river in YB which provides annual mean runoff of  $3.41 \times 10^9$  m<sup>3</sup> (Wang et al.,  
239 2013) and plays an utmost role in protecting the lake and its surrounding ecology and



240 environment. The Dashankou station is the dividing point that divides the mainstream of the  
241 river into middle and lower reaches. In YB, the runoff in Kaidu River is mainly diverted for  
242 agricultural irrigation and finally flows into Bosten Lake, which contributes to about 95% of  
243 the water recharge for the lake (Yao et al., 2018). Bosten Lake is a largest freshwater inland  
244 lake in China covering the area of about 1005 km<sup>2</sup> with a length of 55 km and a width of 25 km.  
245 The lake water volume is approximately  $8.8 \times 10^9$  m<sup>3</sup>, with an average depth of 7 m and a  
246 maximum depth of 17 m (Xiao et al., 2010). The evaporation and an artificial discharge by a  
247 pumping station built in 1983 control the outflow of the lake. As shown in Fig. 2, the pumping  
248 channel starting from the outflow point is utilized to divert the lake water to recharge Kongqi  
249 River and supply water to the lower Tarim River. The dam is built to sustain higher lake level  
250 for the water diversion. Therefore, Bosten Lake is a main water source to the lower reaches of  
251 Tarim River, which had suffered from severe degradation of ecological environment resulted  
252 from unregulated water exploitation in the past few decades. The Chinese government  
253 implemented the Ecological Water Conveyance Project in 2000 to sustain ecosystem in the  
254 lower Tarim River by transferring water from Bosten Lake (Xu et al., 2007; Hao and Li, 2014).  
255 However, YB is an intensive agricultural area where is mostly made up of farmland growing  
256 crops of tomato and pepper. The irrigation water demands accounted for 90% of the total water  
257 consumption in the basin due to the rapid increase of farmland area in the recent years (Yao, et  
258 al., 2018). Consequently, scientific water management strategies should strike for balancing the  
259 demands for existing irrigation and eco-environmental water use to sustain enough water  
260 inflowing from Kaidu River to the lake and the aquifer.

261 This study selects the core part of YB comprising the majority of irrigation districts.  
262 Kaidu River plays a vital role in regulating and maintaining regional water balance in YB. The  
263 modeled domain (Fig. 2) is bounded by the mountains on the northwest, the Huangshuigou  
264 River on the northeast, swamp areas and Bosten Lake on the south. As shown in Fig. 2, an



265 aqueduct system conveys and redistributes the surface runoff from the mainstream of Kaidu  
266 River and the fully penetrating wells are used to pump groundwater from the aquifer.

267 **Figure 2.**

### 268 *3.2 Numerical model*

269 The numerical model in this study is modified from the previous work of Wu et al. (2018)  
270 using MODFLOW-NWT and then performed a multi-objective optimization based on the  
271 corrected model. The specified boundary conditions in the model are illustrated in Fig. 3. The  
272 northwest border was defined as the flow boundary to simulate recharge of groundwater runoff  
273 in the interface between mountains and plain. Huangshuigou River and southwest border were  
274 considered as the specified head boundary based on observed groundwater level. The swamps  
275 and Bosten Lake were modelled using the general head boundary (GHB) package and LAK3  
276 package, respectively. The bathymetric contours of Bosten Lake were used to confirm the lake  
277 bottom topography. Kaidu River and aqueducts were simulated using the SFR2 package. The  
278 simulation period in the transient model was defined from November in 2003 to October in  
279 2013. Totally 20 stress periods were discretized, two periods for each year including  
280 non-irrigation period (from November to next March) and irrigation period (from April to  
281 October of each year), in the entire simulation period. The key model parameters for both SW  
282 and GW were adjusted to reproduce the fluctuation of groundwater levels at the observation  
283 wells and streamflow in the gaging stations (*i.e.*, Yanqi and Baolangsumu stations) as shown in  
284 Fig. 3. The observed lake levels in the simulation period were employed to calibrate the model.

285 **Figure 3.**

286 The model calibration was manually implemented by the trial-and-error method. The  
287 Nash-Sutcliffe Efficiency (NSE) was applied to evaluate the simulated precision of runoff and  
288 lake level. The predicted accuracy of groundwater head was assessed based on root mean



289 square error (RMSE) and correlation coefficient ( $R$ ). The performance criteria can be stated as:

$$290 \quad \text{NSE} = 1 - \frac{\sum_{t=1}^T (y_{m,t} - y_{o,t})^2}{\sum_{t=1}^T (y_{o,t} - \bar{y}_o)^2} \quad (3)$$

$$291 \quad \text{RMSE} = \sqrt{\sum_{i=1}^N (y_{m,i} - y_{o,i})^2 / N} \quad (4)$$

$$292 \quad R = \frac{\sum_{i=1}^N (y_{m,i} - \bar{y}_m)(y_{o,i} - \bar{y}_o)}{\sqrt{\sum_{i=1}^N (y_{m,i} - \bar{y}_m)^2 \times \sum_{i=1}^N (y_{o,i} - \bar{y}_o)^2}} \quad (5)$$

293 where  $y_{m,t}$  and  $y_{o,t}$  are the simulated and observed runoff or lake level for  $t$ th stress period,  
294 respectively;  $T$  is the number of stress periods;  $y_{m,i}$  and  $y_{o,i}$  are the simulated and observed  
295 groundwater head at the  $i$ th observation well, respectively;  $N$  is the number of observation  
296 wells;  $\bar{y}_m$  and  $\bar{y}_o$  are the average value of simulated and observed data. Fig. 4a and 4b  
297 compare the simulated and observed runoff at Yanqi and Baolangsumu Stations for the periods  
298 between 2004 and 2012 and suggest that the long-term fluctuation of runoff in Kaidu River can  
299 be well reproduced by the model. Fig. 4d shows the simulated groundwater heads have a  
300 good-fit with observed heads at the all observation wells with RMSE of 1.8 m and R of 0.98.  
301 Fig. 4e compares the observed and calibrated groundwater level over time in the three  
302 observation wells and the groundwater variation trend in the irrigation and non-irrigation  
303 period can be achieved.

#### 304 **Figure 4.**

305 The interaction between Bosten Lake and the aquifer is dominated by the hydraulic  
306 conductivity of the lakebed, of which value is very small owing to the existence of the thick  
307 low-permeability sediment in the region. The main inflow term of the lake is the surface runoff  
308 from Kaidu River which has been calibrated based on the runoff in the gauging stations. The



309 recharge for the lake from precipitation is not significant in the arid inland basin. The outflow  
310 terms are mainly composed of the evaporation and artificial pumping to divert water from the  
311 lake to Kongqi River. The local water resources authority in YB provided the data of artificial  
312 pumping in the simulation period. However, the average evaporation in Bosten Lake calculated  
313 using potential evaporation data or Penman's equation is not accurate because the temperature  
314 and relative humidity exhibit the significant difference over the approximately 945.0 km<sup>2</sup>  
315 evaporation surface. Therefore, the observed lake stages were applied to calibrate evaporation  
316 rate in the lake. Fig. 4c illustrates the calibration results of lake level and indicates that the  
317 decline trend of lake level can be adequately captured. Then, the water balance of Bosten Lake  
318 can be achieved as shown in Fig. 5. In the simulation period from 2004 to 2013, surface runoff  
319 inflow in Kaidu River represents 97.4% of the total annual inflow to the Bosten Lake. The total  
320 annual outflow of the lake consists of 54.9% of lake evaporation and 44.2% of artificial  
321 pumping. Therefore, the surface runoff in Kaidu River is a crucial factor to maintain the water  
322 balance of Bosten Lake. The surface runoff inflow can be considered as a significant  
323 performance metric to evaluate the water management practices in YB. Finally, the numerical  
324 model has been well-calibrated and can be employed to integrated SW and GW management.

325 **Figure 5.**

### 326 *3.3 Management model*

327 The integrated SW and GW management focuses on not only the water resources  
328 exploitation subject to social and economic benefits but also the effect of water exploitation on  
329 environment benefits. The study formulated an integrated SW and GW optimization problem  
330 including four management objectives: (1) to maximize total water supply rate ( $f_{TWS}$ ); (2) to  
331 minimize total cost of water delivery from water intake points to water use destinations ( $f_{TCOST}$ );  
332 (3) to maximize the groundwater storage change of saturated zone between the beginning and



333 end of management period ( $f_{GSC}$ ) which is negative when the storage decreases and vice versa;  
 334 and (4) to maximize surface runoff inflow from Kaidu River to Bosten Lake ( $f_{SRI}$ ).  $f_{TWS}$  and  
 335  $f_{TCOST}$  are defined as the metrics to satisfy the local irrigation water demands while maintain the  
 336 lower costs of water use.  $f_{GSC}$  is formulated as the metric indicating the extent of groundwater  
 337 exploitation and a greater value shows a preferred situation.  $f_{SRI}$  is defined to evaluate the  
 338 influence of surface runoff from Kaidu River on the water balance in Bosten Lake, which  
 339 contributes about 97.4% of the total inflow (Fig. 5). As shown in Fig. 6, the decision variables  
 340 are the total volume of surface water diverted in the mainstream of Kaidu River in the  
 341 diversion point (DP1-DP7) and groundwater abstraction in the irrigation districts (ID1-ID11).  
 342 The formulations of management model are given as follows:

$$343 \quad \text{Max} \quad f_{TWS} = \sum_{i=1}^{N_p} Q_{g,i} + \sum_{i=1}^{N_d} Q_{s,i} \quad (6)$$

$$344 \quad \text{Min} \quad f_{TCOST} = \sum_{k=1}^{N_t} \sum_{i=1}^{N_w} q_{g,i,k} C_g (H_i - h_{i,k}) T_k + \sum_{k=1}^{N_t} \sum_{i=1}^{N_d} q_{s,i,k} C_s T_k \quad (7)$$

$$345 \quad \text{Max} \quad f_{GSC} = \sum_{j=1}^{N_g} (h_{end,j} - h_{ini,j}) S y_j A_j \quad (8)$$

$$346 \quad \text{Max} \quad f_{SRI} = f_{gaging}(\mathbf{X}) \quad (9)$$

$$347 \quad \mathbf{X} = (Q_{g,1}, Q_{g,2}, \dots, Q_{g,N_p}; Q_{s,1}, Q_{s,2}, \dots, Q_{s,N_d}) \quad (10)$$

348 where  $Q_{g,i}$  is total groundwater abstraction rate at  $i$ th irrigation district ( $\text{m}^3/\text{yr}$ );  $Q_{s,i}$  is total  
 349 volume of surface water diverted from  $i$ th diversion point ( $\text{m}^3/\text{yr}$ );  $N_p$  is the number of  
 350 irrigation districts;  $N_d$  is the number of diversion point based on the locations of aqueducts;  $N_t$   
 351 is the number of stress period including irrigation and non-irrigation period;  $N_w$  is total number  
 352 of pumping wells;  $q_{g,i,k}$  is the pumping rate at the  $i$ th well in  $k$ th stress period ( $\text{m}^3/\text{d}$ );  $C_g$  is the  
 353 cost per unit pumping rate per length of hydraulic lift in case of wells ( $0.015 \text{ CNY}/\text{m}^3/\text{m}$ );  $H_i$  is  
 354 the surface elevation at the  $i$ th pumping well (m);  $h_{i,k}$  is the groundwater level at the  $i$ th well in



355  $k$ th stress period (m);  $T_k$  is the length of the  $k$ th stress period (d);  $q_{s,i,k}$  is the surface water  
 356 diversion rate at the  $i$ th diversion point in  $k$ th stress period ( $\text{m}^3/\text{d}$ );  $C_s$  is the cost per unit  
 357 diversion volume ( $0.055 \text{ CNY}/\text{m}^3$ );  $N_g$  is the total number of active cell in the modelling  
 358 domain;  $h_{end,j}$ ,  $h_{ini,j}$  is the groundwater level at the end and beginning of management period  
 359 (m);  $Sy_j$  is the specific yield at  $j$ th active cell;  $A_j$  is the area of  $j$ th grid cell ( $\text{m}^2$ );  $f_{gaging}$  outputs  
 360 the surface runoff in Kaidu River at the inflow point of Bosten Lake;  $\mathbf{X}$  is a water use scheme.

361 **Figure 6.**

362 The management model consists of a set of constraints given by:

363 
$$Q_{g,min} \leq Q_{g,i} \leq Q_{g,max} \quad Q_{s,min} \leq Q_{s,i} \leq Q_{s,max} \quad (11)$$

364 
$$d_{max} \leq d_c \quad h_{lake} \geq h_c \quad (12)$$

365 
$$\sum_{i=1}^{N_p} Q_{g,i} \geq TP_{min} \quad \sum_{i=1}^{N_d} Q_{s,i} \geq TD_{min} \quad (13)$$

366 
$$Q_{out,i} > 0.0 \quad (14)$$

367 where  $Q_{g,min}$  and  $Q_{g,max}$  are the capacity of total groundwater abstraction at specified irrigation  
 368 district and  $Q_{g,min}$  is uniformly assumed to  $1 \times 10^6 \text{ m}^3/\text{yr}$  and  $Q_{g,max}$  is  $1 \times 10^8 \text{ m}^3/\text{yr}$ ;  $Q_{s,min}$  and  
 369  $Q_{s,max}$  are the constraints of surface water diversion at diversion point,  $Q_{s,min}$  is  $1 \times 10^7 \text{ m}^3/\text{yr}$  at  
 370 diversion points DP1 and DP2 and  $5 \times 10^6 \text{ m}^3/\text{yr}$  at DP3-DP7,  $Q_{s,max}$  is  $4 \times 10^8 \text{ m}^3/\text{yr}$  at DP1 and  
 371  $2 \times 10^8 \text{ m}^3/\text{yr}$  at DP2 and  $1 \times 10^8 \text{ m}^3/\text{yr}$  at DP3-DP7;  $d_{max}$  is the maximum drawdown and must  
 372 less than the permission value  $d_c$  which is set to 5 m based on the existing management  
 373 schemes;  $h_{lake}$  is lake level and must greater than minimum level  $h_c$  (1045 m in this study) to  
 374 divert lake water to recharge Kongqi River;  $TP_{min}$  and  $TD_{min}$  is the prescribed minimum water  
 375 demands of total groundwater abstraction and total surface diversion to satisfy the agricultural  
 376 development and are set to  $3.0 \times 10^8 \text{ m}^3/\text{yr}$  and  $5.5 \times 10^8 \text{ m}^3/\text{yr}$  based on the reports from the  
 377 local water resources authority;  $Q_{out,i}$  represents outflow of the end reach of  $i$ th stream segment





378 and must greater than zeros which means the potential diversion at each diversion point does  
379 not exceed the available streamflow in the current segment to avoid significant error of water  
380 budgets in the optimization (Wu et al., 2015). This study aims at optimizing spatial distribution  
381 of groundwater abstraction at different irrigation district and surface water diversion at each  
382 diversion point. The management period was set to one year with duplicated model inputs and  
383 parameters from November 2012 to October 2013 including the non-irrigation and irrigation  
384 periods. Then the conjunctive management of SW and GW is implemented based on the  
385 multi-objective optimization framework carried out in MATLAB software  
386 (<http://www.mathworks.com/products/matlab>).

## 387 **4 Results and discussion**

### 388 *4.1 Pareto-optimal solutions*

389 This study applied  $\varepsilon$ -MOMA to solve the integrated SW and GW management model with  
390 four objectives ( $f_{TWS}$ ,  $f_{TCOST}$ ,  $f_{GSC}$  and  $f_{SRI}$ ) to search for optimal water use schemes. The  
391 algorithm parameters and objective epsilon values are summarized in Table 1. Fig. 7 shows a  
392 global view of tradeoff surface in a 4-dimensional coordinate plot. The management model  
393 consists of maximizing the  $f_{TWS}$ ,  $f_{GSC}$  and  $f_{SRI}$  objectives and minimizing the  $f_{TCOST}$  objective.  
394 The  $f_{TWS}$ ,  $f_{SRI}$  and  $f_{GSC}$  are plotted on the  $x$ ,  $y$  and  $z$  axes and  $f_{TCOST}$  is represented with color in  
395 Fig. 7. The green arrow indicates the direction of optimality in each objective. It can be  
396 observed that the trade-off relationship exists between  $f_{TWS}$  and other objectives ( $f_{TCOST}$ ,  $f_{GSC}$   
397 and  $f_{SRI}$ ). Augmenting the total amount of water supply increases the cost of transporting water  
398 with the solutions marked in red color and reduces surface runoff inflow to the lake and  
399 groundwater storage at the end of management period. Therefore, the regional water resources  
400 exploitation conflicts with the socioeconomic and environmental benefits in YB. The scheme  
401 before optimization is marked in red square box in Fig. 7. We can see that the scheme is



402 located above the tradeoff surface and exhibits larger cost value. Thus, the current management  
403 scheme is sub-optimal and can be regulated to obtain optimal performances.

404 **Table 1.**

405 **Figure 7.**

406 To explain the discrepancy of the Pareto approximate set, the parallel coordinates plot is  
407 used to illustrate the tradeoff surface while the total pumping rate ( $f_{TPR}$ ) and total surface water  
408 diversion rate ( $f_{TDR}$ ) are added to elucidate the effect of conjunctive use of SW and GW. In Fig.  
409 8, the segments with higher  $f_{TWS}$  exist for higher  $f_{TCOST}$  and lower  $f_{GSC}$  and  $f_{SRI}$ , indicating that  
410 increasing water demands requires more financial investment and depletes more surface runoff  
411 inflow to the lake and groundwater storage. The findings are consistent with the previous  
412 inferences in Fig. 7. Moreover, the many slope segments exist between  $f_{TPR}$  and  $f_{GSC}$ ,  $f_{TDR}$  and  
413  $f_{SRI}$ , which indicates that enlarging groundwater abstraction and surface water diversion are the  
414 dominated factors for the depletion of groundwater storage and surface runoff recharge for the  
415 lake, respectively. It is noteworthy that the variation trend of  $f_{TPR}$  is very close to the change of  
416  $f_{TWS}$  while the change in  $f_{TDR}$  exists obvious difference. The increment of  $f_{TPR}$  can be reached to  
417  $4.16 \times 10^8$  m<sup>3</sup>/yr whereas the growth of  $f_{TDR}$  only is  $1.14 \times 10^8$  m<sup>3</sup>/yr across all the Pareto  
418 solutions. Therefore, groundwater abstraction can be adjusted largely to satisfy management  
419 objectives based decision-makers' preference whereas surface water diversion should be  
420 restricted. The reasons behind this bias are that surface water diversion is highly sensitive to  
421 the lake level and the intensive groundwater abstraction augments the river leakage that  
422 indirectly causes the decrease of the available runoff.

423 **Figure 8.**

#### 424 4.2 Optimized management schedule

425 The superiority in many-objective optimization is the full exploration of optimal solutions



426 to avoid the decision bias derived from the lower dimensional objective formulation. The  
427 decision-makers can firstly analyze the performance of the Pareto solutions in the sub-problem  
428 (e.g., single or two-objective optimization) and then explore the tradeoff solutions using the  
429 previous analysis in the higher order objective space to satisfy the multi-stakeholders' benefits.  
430 Figs. 9a-9c illustrate the projection of four-objective Pareto solutions onto two-objective space  
431 with non-dominated front of the sub-problem constructed by the  $f_{TWS}$  and other objective  
432 ( $f_{TCOST}$ ,  $f_{GSC}$  and  $f_{SRI}$ ), respectively. As shown in Figs. 9a-9c, Solutions 1-3 are the compromise  
433 solutions in the non-dominated front in the two-objective sub-problem which may be selected  
434 by the decision-makers with no preference in the certain objectives. However, these  
435 high-performance solutions in the two-objective optimization exhibit worse performance in the  
436 other objective spaces. As illustrated in the plots (Fig. 9), Solutions 2 and 3 have higher  $f_{TCOST}$   
437 than Solution 1 in Fig. 9a, Solutions 1 and 3 have lower  $f_{GSC}$  than Solution 2 in Fig. 9b and  
438 Solutions 1 and 2 show lower  $f_{SRI}$  than Solution 3 in Fig. 9c. Therefore, the decision-makers  
439 need identify the true compromise solution that performs well in the multiple objectives  
440 simultaneously. In this study, Solution 4 is closest to the corresponding objective values of the  
441 compromise solutions (Solutions 1-3) at the same time and can be a true compromise solution  
442 in the 4-dimensional tradeoff surface. Additionally, Solution 5 has the largest objective value of  
443 total water supply rate in the Pareto approximate set which meets constraints of maximum  
444 groundwater drawdown and minimum lake level. Solution 6 corresponds to the compromise  
445 solution in the non-dominated front of  $f_{GSC}$  and  $f_{SRI}$  which indicates the perfect performance in  
446 the protection of regional groundwater storage and water balance of the lake.

447 **Figure 9.**

448 In this study, Solutions 4, 5 and 6 are selected to elucidate the variation of groundwater  
449 abstraction and surface water diversion compared with the scheme before optimization  
450 (Solution 7). The objective values of selected solutions are listed in Table 2. It can be observed



451 that Solution 4 can achieve similar total water supply rate while the cost of water delivery can  
452 reduce 34.4% compared with Solution 7. The result shows that Solution 7 is sub-optimal from  
453 the aspect of expenditure of water supply. Moreover, the surface runoff inflow to lake in  
454 Solution 4 achieves the increment of  $3.82 \times 10^7$  m<sup>3</sup>/yr and the depletion in groundwater storage  
455 obtains the reduction of  $1.99 \times 10^7$  m<sup>3</sup>/yr. However,  $f_{GSC}$  of Solution 4 is still less than zero  
456 which demonstrates the loss of groundwater storage compared with initial state. Therefore,  
457 Solution 6 is a preferred water use scheme from the aspects of the maximization of  
458 groundwater storage and surface runoff inflow to lake simultaneously. The objectives of  
459 Solution 6 in Table 2 show reducing  $1.43 \times 10^8$  m<sup>3</sup>/yr of  $f_{TWS}$  in the scheme before optimization  
460 can achieve the increment of groundwater storage with  $2.19 \times 10^7$  m<sup>3</sup>/yr and augment  $6.30 \times 10^7$   
461 m<sup>3</sup>/yr of surface runoff inflow to lake. Solution 5 represents the potential of water resources  
462 exploitation in YB and can augment 26% of total water supply rate compared with Solution 7.  
463 Interestingly, it can be found that, in Solutions 5 and 7, groundwater storage depletion  
464 ( $8.39 \times 10^7$  m<sup>3</sup>/yr) is more rapid than the reduction of surface runoff inflow to the lake ( $1.85 \times 10^7$   
465 m<sup>3</sup>/yr), which indicates groundwater abstraction is probably preferred option to provide the  
466 resiliency of water supply in the face of the increased water demands.

467 **Table 2.**

468 Fig. 10 illustrated the spatial distribution of the pumping rates of the selected solutions at  
469 11 irrigation districts. As shown in Figs. 10a and 10b, Solution 4 shows groundwater  
470 abstraction in the ID3, ID5 and ID7-ID11 can be increased in comparison to Solution 7. It can  
471 be noted that the pumping rates in ID7 and ID9 can be largely elevated due to lower  
472 exploitation in the past and shallow groundwater depth. The groundwater abstraction in ID1,  
473 ID2, ID4 and ID6 should be reduced especially for the pumping rate in ID6 which exhibits  
474 abrupt decline. As shown in Fig. 10c, Solution 5 with the maximization of  $f_{TWS}$  demonstrates  
475 that a large amount of groundwater can be abstracted in the ID5-ID9 (greater than  $8 \times 10^7$  m<sup>3</sup>/yr)



476 which implies water managers can implement groundwater abstraction in those districts to  
477 satisfy the augmentation of water supply. In Fig. 10d, Solution 6 is a desired scheme with the  
478 maximization of environment benefits in groundwater storage and runoff recharge to the lake.  
479 The spatial differentiation of groundwater abstraction in Solution 6 is similar with those in the  
480 4-dimensional compromise solution (Solution 4). However, Solution 6 based the pumping rates  
481 in the ID5 and ID8 show obvious decline, which implies that water managers can lower the  
482 groundwater abstraction in these regions to achieve more environment benefit in groundwater  
483 storage.

484 **Figure 10.**

485 Fig. 11 illustrates the spatial patterns of surface water diversion along the main stream of  
486 Kaidu River. As show in Fig. 11a, seven diversion points (DP1-DP7) with the reduction of  
487 runoff are clearly identified. The runoff at the 35 km from DP1 exhibits obvious rise due to the  
488 inflow in the tributary. The river runoff at the lake inflow point is the surface runoff inflow to  
489 the lake that is  $f_{SRI}$  objective. It can be observed that the surface runoff in the scheme before  
490 optimization (Solution 7) in DP1 shows the abrupt decline than Pareto-optimal solutions  
491 (Solutions 4, 5 and 6) which responds to the distribution of surface diversion in Fig. 11b.  
492 Moreover, Solution 7 has the lowest runoff between DP1 and DP4 even though exists slight  
493 increase in the lake inflow point. Therefore, a significant increase of surface water diversion in  
494 DP1 controls the available runoff in the downstream segments. The water managers should  
495 reduce the surface water diversion in DP1 to ensure sufficient runoff in the lower reaches of  
496 Kaidu River for the adjustment of multi-stakeholders' benefits. Solution 4 is a compromise  
497 scheme that exhibits lower runoff compared with Solution 6 from DP4 to the end of river, due  
498 to the larger water diversion in DP4, which triggers the reduction of surface runoff inflow to  
499 lake. Solution 5 is a potential of regional water resources exploitation in YB and has smaller  
500 available runoff than Solutions 4 and 6 which implement more water diversion in Kaidu River.



501 Fig. 11c further demonstrates the interaction of surface water and groundwater along the  
502 mainstream of the river. The upper segment (Segment I) is a losing segment that means surface  
503 water exchange from stream to aquifer and the middle segment (Segment II) is a gaining  
504 segment that indicates groundwater exchange from aquifer to stream. Then the lower segment  
505 (Segment III) turns into a losing segment. It can be noted that Segment I and Segment II have  
506 strong interaction between SW and GW whereas Segment III exhibits exchange with a lower  
507 leakage rate. As illustrated in Fig. 11d, the distribution of total river leakage shows Solution 5  
508 maximizing water supply corresponds to the maximum loss of runoff which is in fact caused  
509 by the substantial groundwater abstraction and the exchange from Solutions 6 and 7 shows the  
510 less river leakage. Consequently, groundwater abstraction is a dominated factor for the  
511 interaction of SW and GW for the YB water management. The river leakage in Solution 4 is  
512 obviously larger than Solution 7 which is seemingly undesired for water managers. However,  
513 augmenting groundwater abstraction ( $1.31 \times 10^8 \text{ m}^3/\text{yr}$ ) at the cost of river leakage ( $0.30 \times 10^8$   
514  $\text{m}^3/\text{yr}$ ) can lower surface water diversion ( $0.67 \times 10^8 \text{ m}^3/\text{yr}$ ) directly from the river that is highly  
515 sensitive to the runoff inflow to Bosten Lake. Therefore, groundwater abstraction is probably a  
516 desired water use pattern in YB.

517 **Figure 11.**

#### 518 *4.3 Impacts of runoff change*

519 Kaidu River plays a crucial role to sustain regional water balance in YB and flows through  
520 Dashankou station (Fig. 2) into the basin. The river supplies the majorities of surface water  
521 diversion by an aqueduct system for agricultural irrigation and constitutes about 95% of total  
522 annual inflow to the Bosten Lake. The runoff in Kaidu River is mainly originated from  
523 mountainous precipitation and melting glacier water in the Tianshan Mountains region.  
524 However, the remarkable climate changes have caused a significant increase in both



525 temperature and precipitation over the past 50 years in Xinjiang (Li et al., 2013). The changing  
526 climate probably increased the glacier melt and snowmelt in the upper part of Kaidu River and  
527 then caused the growth of the river runoff between 1999 and 2002, with the highest runoff in  
528 2002 of 5.7 billion m<sup>3</sup>/year (Zhou et al., 2015). However, the long-term climate change may  
529 reduce runoff in Kaidu River attributing to the depletion of small or mid-size glaciers and snow  
530 line receding in the middle Tianshan Mountains region. Li et al., (2012) observed that surface  
531 area of snow in the Kaidu River Basin reduced largely between 2000 and 2010. Therefore, it is  
532 essential to consider the impact of runoff reduction in Kaidu River on the regional water  
533 resources management for the local socioeconomic and environmental development.

534 This study implemented multi-objective optimization by resetting the runoff inflow at the  
535 first diversion point (DP1) in Kaidu River with the duplicated model parameters and the inputs  
536 of source and sink terms. We defined three scenarios which are to maintain the current runoff  
537 (Scenario A0), reduce 10% of the runoff (Scenario A1) and reduce 20% of the runoff (Scenario  
538 A2), respectively. In the management model, the constraint of lake level is altered to the  
539 smaller value (1044.5m) and maximum groundwater drawdown is reset to 10m to avoid much  
540 more infeasible solutions in the population which probably inhibits the convergence of the  
541 optimization. The hypervolume metric (HV) is used to evaluate the convergence of  
542 Pareto-optimal solutions under the three scenarios. The advantage of HV is the monotonically  
543 increasing relationship between the metric value and Pareto dominance, which shows the  
544 optimal tradeoff surface can achieve maximum hypervolume (Bader and Zitzler, 2011). Fig. 12  
545 shows all Pareto-optimal solutions in the four-dimensional objective space under different  
546 runoff change scenarios. It is obviously observed that the tradeoff surface with current runoff  
547 (Scenario A0) is closest to the ideal solution and those with runoff reduction are farther from  
548 the solution. Scenario A2 based solutions exhibit worst performance owing to the greatest  
549 extent of runoff reduction. Moreover, we rescaled the objective range to the interval [0, 1] and



550 set the reference point to the objective vector (1, 1, 1, 1) to calculate the HV metric. Fig. 13  
551 shows the evolution of HV and the number of generation. Judged from the performance  
552 evolution, tradeoff solutions under Scenario A0 achieve the largest HV and those in Scenario  
553 A2 have the lowest HV that shows the solutions are far away from the Pareto-optimal front.  
554 Therefore, the exploitation extent of surface diversion and groundwater abstraction should be  
555 diminished in the face of runoff reduction derived from climate change. In Fig. 12,  
556 Pareto-optimal solutions in Scenarios A1 and A2 does not exists when  $f_{SRI}$  is greater than a  
557 certain value and the diversity of solutions is obviously decreased. The reason is that  
558 augmenting  $f_{TWS}$  causes more decline of  $f_{SRI}$  and the lake level compared with no reduction in  
559 runoff in Scenario A0, which more likely generates a large amount of unfeasible solutions  
560 violating the constraint of minimum lake level. The finding also shows that runoff in Kaidu  
561 River through YB is a dominant factor controlling the variation of Bosten Lake level. To  
562 investigate the effect of runoff reduction on the environmental benefits, Fig. 14 shows the  
563 non-dominated fronts in the  $f_{GSC}$  and  $f_{SRI}$  objectives space across Scenarios A0, A1 and A2. The  
564 solutions in Scenario A2 are completely dominated by the solutions in Scenarios A0 and A1.  
565 Scenario A0 based solutions show the best Pareto optimality. Therefore, the runoff reduction  
566 results in dramatic loss of environmental benefits. It is noteworthy that  $f_{SRI}$  with Scenarios A1  
567 and A2 will be reduced under the similar  $f_{GSC}$ . In the optimization, in order to maximize  
568 irrigation water supply, sustaining similar groundwater storage in Scenarios A1 and A2 has to  
569 be at the cost of river runoff decline to augment surface water diversion. Consequently, it is  
570 essential for water managers to realize the conflict of conjunctive use of SW and GW for the  
571 water management in arid inland basin.

572 **Figure 12.**

573 **Figure 13.**

574 **Figure 14.**





575 **5. Conclusions**

576 The study proposed a multi-objective optimization framework for the integrated surface  
577 water and groundwater management and demonstrated its effectiveness through a spatial  
578 optimization of water use practices for the agricultural irrigation in Yanqi Basin, a typical arid  
579 inland basin in northwest China. The well-calibrated simulation model with MODFLOW-NWT  
580 was developed to model the interaction of surface water (*i.e.*, Kaidu River and Bosten Lake)  
581 and groundwater. Then this study presented a new MOEA (the epsilon multi-objective memetic  
582 algorithm,  $\epsilon$ -MOMA) and linked it with the numerical model to solve the multi-objective  
583 management model. The optimization model is composed of the four conflicting objectives:  
584 maximizing total water supply rate, minimizing total cost of transporting water from water  
585 intake points to water use destinations, maximizing the groundwater storage change in the  
586 aquifer and maximizing the surface runoff inflow from Kaidu River to Bosten Lake. An  
587 interactive visualization tool was applied to explore 4-dimensional tradeoff surface in a global  
588 view. Results showed augmenting water supply caused the larger cost of water delivery,  
589 reduced the runoff inflow to lake and aggravated the loss of groundwater storage. The  
590 2-dimensional compromise schemes selected from the non-dominated fronts between  $f_{TWS}$  and  
591 other objectives exhibited significant decision bias in the higher order objective spaces.  
592 Therefore, it is essential for decision-makers to explore water management schemes in the  
593 many-objective tradeoff surface.

594 The 4-dimensional compromise solutions were obtained to investigate performance of  
595 existing scheme. Result showed the water use practices before optimization must be regulated  
596 to avoid unnecessary capital expenditure of transporting water. However, the compromised  
597 solution indicated groundwater storage was still decreasing. Thus, the water managers may be  
598 inclined to adopt the Pareto-optimal scheme satisfying minimum water demands to prevent the  
599 loss of groundwater storage and runoff inflow to the lake. In the practical application, the



600 decision-makers should identify specific irrigation water demands and environmental  
601 constraints to discover preferred water use schemes. The scenarios of runoff change were  
602 created to investigate the effect of runoff reduction in Kaidu River on the regional water  
603 resources management. The findings showed that reducing runoff inflow to YB could lead to  
604 the degradation of Pareto solutions compared with those based on the current runoff scenario.  
605 In this light, it is of crucial importance to implement stringent water management schemes and  
606 explore potential water-saving strategies in the face of the uncertainty.

607       The findings in the study are essential to regional water resources management in a typical  
608 arid inland basin with long-term intensive agricultural development. However, due to the  
609 data-scarcity in the basin-scale water cycle and limitations of simulation model, the current  
610 model may be not enough to reflect the complex relationship in the groundwater-river-lake  
611 hydrological system. Future research should focus on exploiting fully coupled numerical model  
612 to accurately simulate basin-scale water cycle and avoid decision bias derived from the  
613 numerical model. Meanwhile, deep uncertainty (*e.g.*, land use change, climate change, etc.) is a  
614 key factor to affect the robustness and reliability of the optimal solutions in the changing world.  
615 In the simulation-optimization framework, integrating these factors into the management  
616 model to explore optimal schemes is a research focus in the future.

### 617 **Acknowledgements**

618       This study is jointly supported by the National Natural Science Foundation of China  
619 (41730856 and 41772254) and the National Key Research and Development Plan of China  
620 (2016YFC0402800). The numerical calculations in this study have been implemented on the  
621 IBM Blade cluster system in the High Performance Computing Center of Nanjing University.

### 622 **References**

623 Bader, J., Zitzler, E.: HypE: an algorithm for fast hypervolume-based many-objective



- 624 optimization, *Evol. Comput.*, 19(1), 45-76, [doi:10.1162/EVCO\\_a\\_00009](https://doi.org/10.1162/EVCO_a_00009), 2011.
- 625 Beh, E.H., Zheng, F., Dandy, G.C., Maier, H.R., and Kapelan, Z.: Robust optimization of water  
626 infrastructure planning under deep uncertainty using metamodels, *Environ. Model.*  
627 *Softw.*, 93, 92-105, [doi:10.1016/j.envsoft.2017.03.013](https://doi.org/10.1016/j.envsoft.2017.03.013), 2017.
- 628 Chen, B., Zeng, W.H., Lin, Y.B., and Zhang, D.F.: A new local search-based multiobjective  
629 optimization algorithm, *IEEE Trans.*, 19(1), 50-73, [doi:10.1109/TEVC.2014.2301794](https://doi.org/10.1109/TEVC.2014.2301794),  
630 2015.
- 631 Deb, K., Pratap, A., Agarwal, S., and Meyerivan, T.: A fast and elitist multi-objective genetic  
632 algorithm: NSGA-II, *IEEE Trans.*, 6(2), 182-197, [doi:10.1109/4235.996017](https://doi.org/10.1109/4235.996017), 2002.
- 633 Eker, S., and Kwakkel, J.H.: Including robustness considerations in the search phase of  
634 Many-Objective Robust Decision Making, *Environ. Model. Softw.*, 105, 201-216,  
635 [doi:10.1016/j.envsoft.2018.03.029](https://doi.org/10.1016/j.envsoft.2018.03.029), 2018.
- 636 Gao, H., and Yao, Y.: Quantitative effect of human activities on water level change of Bosten  
637 Lake in recent 50 years, *Scientia Geographica Sinica*, 25, 3305-3309, 2005 (in Chinese  
638 with English abstract).
- 639 Hadka, D., Herman, J., Reed, P., and Keller, K.: An open source framework for many objective  
640 robust decision making, *Environ. Model. Softw.*, 74, 114-129,  
641 [doi:10.1016/j.envsoft.2015.07.014](https://doi.org/10.1016/j.envsoft.2015.07.014), 2015.
- 642 Hadka, D., and Reed, P.M.: Brog: an auto-adaptive many-objective framework, *Evol. Comput.*,  
643 21(2), 213-259, [doi:10.1162/EVCO\\_a\\_00075](https://doi.org/10.1162/EVCO_a_00075), 2013.
- 644 Hao, X., and Li, W.: Impacts of ecological water conveyance on groundwater dynamics and  
645 vegetation recovery in the lower reaches of the Tarim River in northwest China, *Environ.*  
646 *Monit. Assess.*, 186(11), 7605-7616, [doi:10.1007/s10661-014-3952-x](https://doi.org/10.1007/s10661-014-3952-x), 2014.
- 647 Hassanzadeh, E., Elshorbagy, A., Wheeler, H., and Gober, P.: Managing water in complex  
648 systems: An integrated water resources model for Saskatchewan, Canada, *Environ.*



- 649 Model. Softw., 58, 12-26, [doi:10.1016/j.envsoft.2014.03.015](https://doi.org/10.1016/j.envsoft.2014.03.015), 2014.
- 650 Hu, L.T., Chen, C.X., Jiao, J.J., and Wang, Z.J.: Simulated groundwater interaction with rivers  
651 and springs in the Heihe river basin, Hydrol. Process., 21(20), 2794-2806,  
652 [doi:10.1002/hyp.6497](https://doi.org/10.1002/hyp.6497), 2007.
- 653 Inselberg, A.: Parallel Coordinates: Visual Multidimensional Geometry and Its Applications,  
654 Springer, New York, USA, [doi:10.1007/978-0-387-68628-8](https://doi.org/10.1007/978-0-387-68628-8), 2009.
- 655 Kasprzyk, J.R., Reed, P.M., Characklis, G.W., and Kirsch, B.R.: Many-objective *de Novo* water  
656 supply portfolio planning under deep uncertainty, Environ. Model. Softw., 34, 87-104,  
657 [doi:10.1016/j.envsoft.2011.04.003](https://doi.org/10.1016/j.envsoft.2011.04.003), 2012.
- 658 Kasprzyk, J.R., Reed, P.M., and Hadka, D.M.: Battling arrow's paradox to discover robust  
659 water management alternatives, J. Water Resour. Plan. Manag., 142(2), 04015053,  
660 [doi:10.1061/\(ASCE\)WR.1943-5452.0000572](https://doi.org/10.1061/(ASCE)WR.1943-5452.0000572), 2015.
- 661 Khare, D., Jat, M.K., and Ediwahyunan.: Assessment of conjunctive use planning options: a  
662 case study of Sapon irrigation command area of Indonesia, J. Hydrol., 328(3-4), 764-777,  
663 [doi:10.1016/j.jhydrol.2006.01.018](https://doi.org/10.1016/j.jhydrol.2006.01.018), 2006.
- 664 Kollat, J.B., and Reed, P.: A framework for visually interactive decision-making and design  
665 using evolutionary multi-objective optimization (VIDEO), Environ. Model. Softw., 22  
666 (12), 1691-1704, [doi:10.1016/j.envsoft.2007.02.001](https://doi.org/10.1016/j.envsoft.2007.02.001), 2007.
- 667 Laumanns, M., Thiele, L., Deb, K., and Zitzler, E.: Combining convergence and diversity in  
668 evolutionary multi-objective optimization, Evol. Comput., 10(3), 263-282,  
669 [doi:10.1162/106365602760234108](https://doi.org/10.1162/106365602760234108), 2002.
- 670 Li, B., Chen, Y., Shi, X., Chen, Z., and Li, W.: Temperature and precipitation changes in  
671 different environments in the arid region of northwest China, Theor. Appl. Climatol., 112,  
672 589-596, [doi:10.1007/s00704-012-0753-4](https://doi.org/10.1007/s00704-012-0753-4), 2013.
- 673 Li, Q., Li, L.H., and Bao, A.M.: Snow cover change and impact on streamflow in the Kaidu



- 674 River Basin, Resources Science, 34, 91-97, 2012 (in Chinese with English abstract).
- 675 Liu, L., Luo, Y., He, C., Lai, J., and Li, X.: Roles of the combined irrigation, drainage, and  
676 storage of the canal network in improving water reuse in the irrigation districts along the  
677 lower Yellow River, China, J. Hydrol., 391(1-2), 157-174,  
678 [doi:10.1016/j.jhydrol.2010.07.015](https://doi.org/10.1016/j.jhydrol.2010.07.015), 2010.
- 679 Liu, L., Zhao, J., Zhang, J., Peng, W., Fan, J., and Zhang, T.: Water balance of Lake Bosten  
680 using annual water-budget method for the past 50 years, Arid Land Geography, 36, 33-40,  
681 2013 (in Chinese with English abstract).
- 682 Maier, H.R., Kapelan, Z., Kasprzyk, J., Kollat, J., Matott, L.S., Cunha, M.C., Dandy, G.C.,  
683 Gibbs, M.S., Keedwell, E., Marchi, A., Ostfeld, A., Savic, D., Solomatine, D.P., Vrugt,  
684 J.A., Zecchin, A.C., Minsker, B.S., Barbour, E.J., Kuczera, G., Pasha, F., Castelletti, A.,  
685 Giuliani, M., and Reed, P.M.: Evolutionary algorithms and other metaheuristics in water  
686 resources: current status, research challenges and future directions, Environ. Model.  
687 Softw., 62, 271-299, [doi:10.1016/j.envsoft.2014.09.013](https://doi.org/10.1016/j.envsoft.2014.09.013), 2014.
- 688 Mamat, Z., Yimit, H., Ji, R.Z.A., and Eziz, M.: Source identification and hazardous risk  
689 delineation of heavy metal contamination in Yanqi basin, northwest China, Sci. Total  
690 Environ., 493, 1098-1111, [doi:10.1016/j.scitotenv.2014.03.087](https://doi.org/10.1016/j.scitotenv.2014.03.087), 2014.
- 691 Matteo, M.D., Maier, H.R., and Dandy, G.C.: Many-objective portfolio optimization approach  
692 for stormwater management project selection encouraging decision maker buy-in,  
693 Environ. Model. Softw., 111, 340-355, [doi:10.1016/j.envsoft.2018.09.008](https://doi.org/10.1016/j.envsoft.2018.09.008), 2019.
- 694 McPhee, J., and Yeh, W.W.G.: Multiobjective optimization for sustainable groundwater  
695 management in semiarid regions, J. Water Resour. Plan. Manag., 130(6), 490-497,  
696 [doi:10.1061/\(ASCE\)0733-9496\(2004\)130:6\(490\)](https://doi.org/10.1061/(ASCE)0733-9496(2004)130:6(490)), 2004.
- 697 Michael, L.M., and Leonard, F.K.: Documentation of a Computer Program to Simulate  
698 Lake-aquifer Interaction Using the Modflow Ground-water Flow Model and the Moc3d



- 699 Solute-transport Model, U.S. Geological Water-Resources Investigations Report, 2000.
- 700 Niswonger, R.G., Panday, S., and Ibaraki, M.: MODFLOW-NWT, A Newton formulation for  
701 MODFLOW-2005: US Geological Survey Techniques and Methods 6-A37, 44 p, 2011.
- 702 Parsapour-Moghaddam, P., Abed-Elmdoust, A., and Kerachian, R.: A heuristic evolutionary  
703 game theoretic methodology for conjunctive use of surface and groundwater resources,  
704 Water Resour. Manag., 29(11), 3905-3918, [doi:10.1007/s11269-015-1035-6](https://doi.org/10.1007/s11269-015-1035-6), 2015.
- 705 Purshouse, R.C., and Fleming, P.J.: On the evolutionary optimization of many conflicting  
706 objectives, IEEE Trans., 11(6), 770-784, [doi:10.1109/TEVC.2007.910138](https://doi.org/10.1109/TEVC.2007.910138), 2007.
- 707 Richard, G.N., and David, E.P.: Documentation of the Streamflow-Routing (SFR2) Package to  
708 Include Unsaturated Flow Beneath Streams-A Modification to SFR1, U.S. Geological  
709 Survey Techniques and Methods, pp. 6-A13, 2010.
- 710 Rothman, D., and Mays, L.W.: Water resources sustainability: development of a  
711 multi-objective optimization model, J. Water Resour. Plan. Manag., 140(12), 04014039,  
712 [doi:10.1061/\(ASCE\)WR.1943-5452.0000425](https://doi.org/10.1061/(ASCE)WR.1943-5452.0000425), 2013.
- 713 Safavi, H.R., and Esmikhani, M.: Conjunctive use of surface water and groundwater:  
714 application of support vector machines (SVMs) and genetic algorithms, Water Resour.  
715 Manag., 27(7), 2623-2644, [doi:10.1007/s11269-013-0307-2](https://doi.org/10.1007/s11269-013-0307-2), 2013.
- 716 Sindhya, K., Deb, K., and Miettinen, K.: Improving convergence of evolutionary  
717 multiobjective optimization with local search: a concurrent-hybrid algorithm, Nat.  
718 Comput., 10(4), 1407-1430, [doi:10.1007/s11047-011-9250-4](https://doi.org/10.1007/s11047-011-9250-4), 2011.
- 719 Sindhya, K., Miettinen, K., and Deb, K.: A hybrid framework for evolutionary multiobjective  
720 optimization. IEEE Trans., 17(4), 495-511, [doi:10.1109/TEVC.2012.2204403](https://doi.org/10.1109/TEVC.2012.2204403), 2013.
- 721 Singh, A.: Simulation-optimization modeling for conjunctive water use management, Agric.  
722 Water Manag., 141, 23-29, [doi:10.1016/j.agwat.2014.04.003](https://doi.org/10.1016/j.agwat.2014.04.003), 2014.
- 723 Singh, A., and Panda, S.N.: Optimization and simulation modelling for managing the problems



- 724 of water resources, *Water Resour. Manag.*, 27(9), 3421-3431,  
725 [doi:10.1007/s11269-013-0355-7](https://doi.org/10.1007/s11269-013-0355-7), 2013.
- 726 Tian, Y., Zheng, Y., Wu, B., Wu, X., Liu, J., and Zheng, C.: Modeling surface  
727 water-groundwater interaction in arid and semi-arid regions with intensive agriculture,  
728 *Environ. Model. Softw.*, 63, 170-184, [doi:10.1016/j.envsoft.2014.10.011](https://doi.org/10.1016/j.envsoft.2014.10.011), 2015.
- 729 Wang, W., Wang, X., Jiang, F., and Peng, D.: Response of runoff volume to climate change in  
730 the Kaidu River Basin in recent 30 years, *Arid Zone research*, 30, 743-748, 2013 (in  
731 Chinese with English abstract).
- 732 Wang, Y., Chen, Y., and Li, W.: Temporal and spatial variation of water stable isotopes ( $^{18}\text{O}$  and  
733  $^2\text{H}$ ) in the Kaidu River basin, Northwest China, *Hydrol. Process.*, 28(3), 653-661,  
734 [doi:10.1002/hyp.9622](https://doi.org/10.1002/hyp.9622), 2014.
- 735 Wichelns, D., and Oster, J.D.: Sustainable irrigation is necessary and achievable, but direct  
736 costs and environmental impacts can be substantial, *Agric. Water Manag.*, 86(1-2),  
737 114-127, [doi:10.1016/j.agwat.2006.07.014](https://doi.org/10.1016/j.agwat.2006.07.014), 2006.
- 738 Woodruff, M.J., Reed, P.M., and Simpson, T.W.: Many objective visual analytics: rethinking  
739 the design of complex engineered systems, *Struct. Multidisc. Optim.*, 48(1), 201-219,  
740 [doi:10.1007/s00158-013-0891-z](https://doi.org/10.1007/s00158-013-0891-z), 2013.
- 741 Wu, B., Zheng, Y., Tian, Y., Wu, X., Yao, Y., Han, F., Liu, J., and Zheng, C.: Systematic  
742 assessment of the uncertainty in integrated surface water-groundwater modeling based on  
743 the probabilistic collocation method, *Water Resour. Res.*, 50, 5848-5865,  
744 [doi:10.1002/2014WR015366](https://doi.org/10.1002/2014WR015366), 2014.
- 745 Wu, B., Zheng, Y., Wu, X., Tian, Y., Han, F., Liu, J., and Zheng, C.: Optimizing water  
746 resources management in large river basins with integrated surface water-groundwater  
747 modeling: A surrogate-based approach, *Water Resour. Res.*, 51, 2153-2173,  
748 [doi:10.1002/2014WR016653](https://doi.org/10.1002/2014WR016653), 2015.



- 749 Wu, M., Wu, J., Lin, J., Zhu, X., Wu, J., and Hu, B.X.: Evaluating the interactions between  
750 surface water and groundwater in the arid mid-eastern Yanqi Basin, northwest China,  
751 *Hydrolog. Sci. J.*, 63(9), 1313-1331, [doi:10.1080/02626667.2018.1500744](https://doi.org/10.1080/02626667.2018.1500744), 2018.
- 752 Wu, X., Zheng, Y., Wu, B., Tian, Y., Han, F., and Zheng, C.M.: Optimizing conjunctive use of  
753 surface water and groundwater for irrigation to address human-nature water conflicts: A  
754 surrogate modeling approach, *Agric. Water Manag.*, 163, 380-392,  
755 [doi:10.1016/j.agwat.2015.08.022](https://doi.org/10.1016/j.agwat.2015.08.022), 2016.
- 756 Xiao, M., Wu F., Liao, H., Li, W., Lee, X., and Huang, R.: Characteristics and distribution of  
757 low molecular weight organic acids in the sediment porewaters in Bosten Lake, China, *J.*  
758 *Environ. Sci.*, 22(3), 328-337, [doi:10.1016/S1001-0742\(09\)60112-1](https://doi.org/10.1016/S1001-0742(09)60112-1), 2010.
- 759 Xu, H., Ye, M., Song, Y., and Chen, Y.: The natural vegetation responses to the groundwater  
760 change resulting from ecological water conveyances to the lower Tarim River, *Environ.*  
761 *Monit. Assess.*, 131(1-3), 37-48, [doi:10.1007/s10661-006-9455-7](https://doi.org/10.1007/s10661-006-9455-7), 2007.
- 762 Xu, J., Chen, Y., Bai, L., and Xu, Y.: A hybrid model to simulate the annual runoff of the Kaidu  
763 River in northwest China, *Hydrol. Earth Syst. Sci.*, 20, 1447-1457,  
764 [doi:10.5194/hess-20-1447-2016](https://doi.org/10.5194/hess-20-1447-2016), 2016.
- 765 Yang, C.C., Chang, L.C., Chen, C.S., and Yeh, M.S.: Multi-objective planning for conjunctive  
766 use of surface and subsurface water using genetic algorithm and dynamics programming.  
767 *Water Resour. Manag.*, 23(3), 416-437, [doi:10.1007/s11269-008-9281-5](https://doi.org/10.1007/s11269-008-9281-5), 2009.
- 768 Yao, J., Chen, Y., Zhao, Y., and Yu, X.: Hydro climatic changes of Lake Bosten in Northwest  
769 China during the last decades, *Scientific Reports*, 8, 9118,  
770 [doi:10.1038/s41598-018-27466-2](https://doi.org/10.1038/s41598-018-27466-2), 2018.
- 771 Yao, Y., Zheng, C., Liu, J., Cao, G., Xiao, H., Li, H., and Li, W.: Conceptual and numerical  
772 models for groundwater flow in an arid inland river basin, *Hydrol. Process.*, 29,  
773 1480-1492, [doi:10.1002/hyp.10276](https://doi.org/10.1002/hyp.10276), 2015.





774 Zhang, Z., Hu, H., Tian, F., Yao, X., and Sivapalan, M.: Groundwater dynamics under  
775 water-saving irrigation and implications for sustainable water management in an oasis:  
776 Tarim River basin of western China, Hydrol. Earth Syst. Sci., 18, 3951-3967,  
777 [doi:10.5194/hess-18-3951-2014](https://doi.org/10.5194/hess-18-3951-2014), 2014.

778 Zhou, H., Cheng, Y., Perry, L., and Li, W.: Implications of climate change for water  
779 management of an arid inland lake in Northwest China, Lake and Reservoir Management.  
780 31(3), 202-213, [doi:10.1080/10402381.2015.1062834](https://doi.org/10.1080/10402381.2015.1062834), 2015.

781

782

783



784 **Tables**

785 Table 1 The control parameters of  $\epsilon$ -MOMA and epsilon value of objectives

| Parameter                                  | Value           |
|--|-----------------|
| Population size ( $N_{pop}$ )              | 200             |
| Maximum function evaluation ( $N_{eval}$ ) | $6 \times 10^4$ |
| Crossover probability ( $P_c$ )            | 0.90            |
| Mutation probability ( $P_m$ )             | 0.05            |
| $f_{TWS}$ epsilon ( $m^3/yr$ )             | $1 \times 10^4$ |
| $f_{TCOST}$ epsilon (CNY/yr)               | $1 \times 10^2$ |
| $f_{GSC}$ epsilon ( $m^3/yr$ )             | $1 \times 10^4$ |
| $f_{SRI}$ epsilon ( $m^3/yr$ )             | $1 \times 10^4$ |

786

787



788 Table 2 The objective values corresponding to several solutions

| Objective                                       | Solution 4 | Solution 5 | Solution 6 | Solution 7 |
|---|------------|------------|------------|------------|
| $f_{TWS} (\times 10^8 \text{ m}^3/\text{yr})$   | 10.7406    | 12.7355    | 8.6712     | 10.1032    |
| $f_{TCOST} (\times 10^6 \text{ CNY}/\text{yr})$ | 54.3013    | 92.1498    | 42.9522    | 82.7827    |
| $f_{GSC} (\times 10^8 \text{ m}^3/\text{yr})$   | -0.2471    | -1.2856    | 0.2192     | -0.4462    |
| $f_{SRI} (\times 10^8 \text{ m}^3/\text{yr})$   | 17.5698    | 17.0030    | 17.8180    | 17.1880    |

789

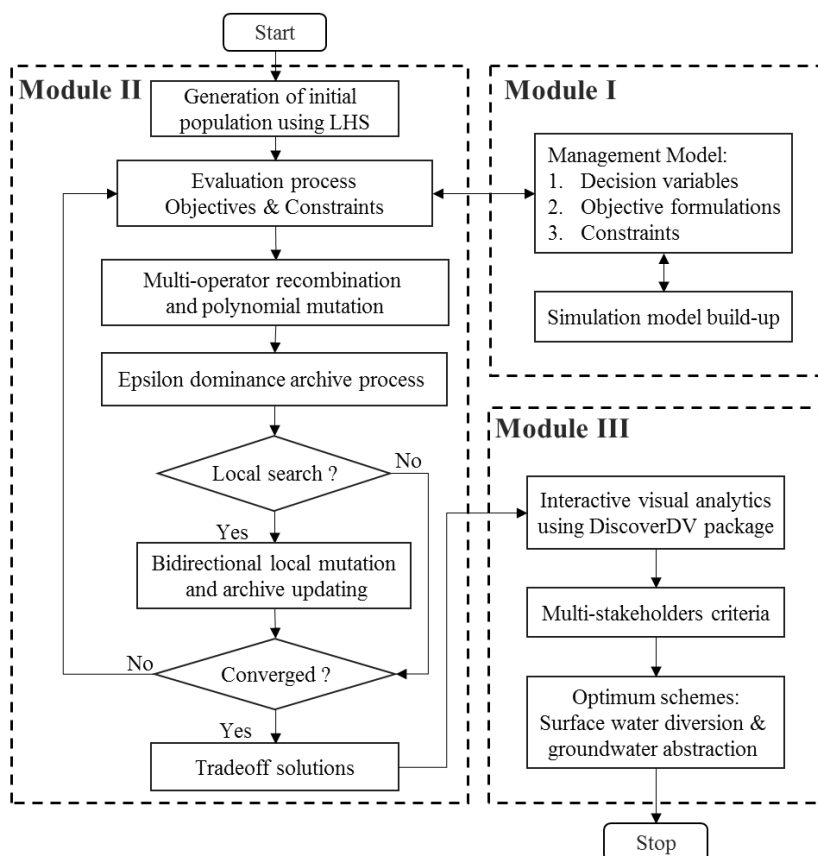
790

791

792



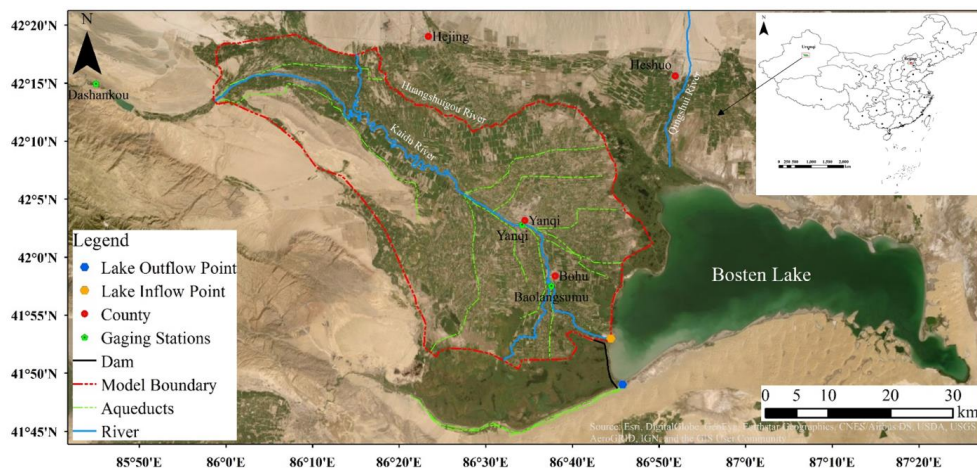
793 **Figures**



794

795 **Fig. 1.** Framework of multi-objective optimization for integrated SW-GW management.

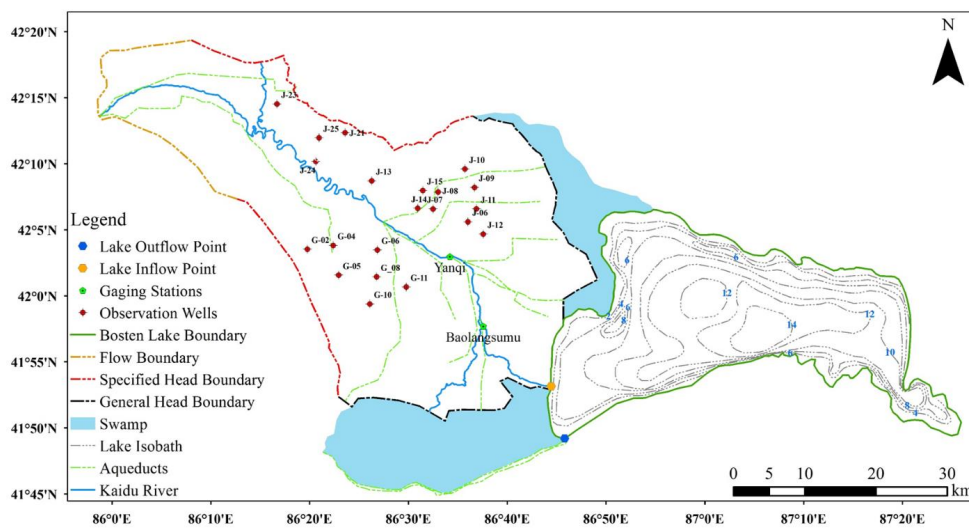
796



797

798 **Fig. 2.** The location of Yanqi Basin and the model domain of interest for this study. Source:  
799 DigitalGlobal, Inc. (imagery).

800

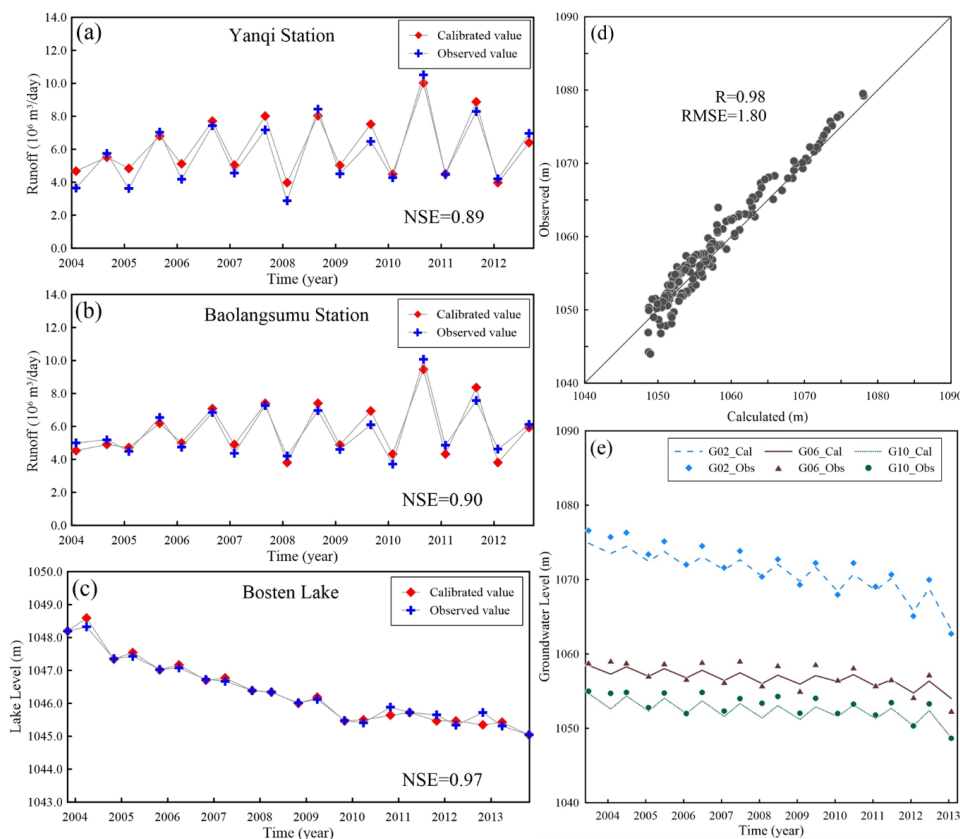


801

802 **Fig. 3.** The boundary conditions of model domain, monitoring locations of groundwater level  
803 and surface runoff, aqueduct system and bathymetric contours in meters for Bosten  
804 Lake.

805

806

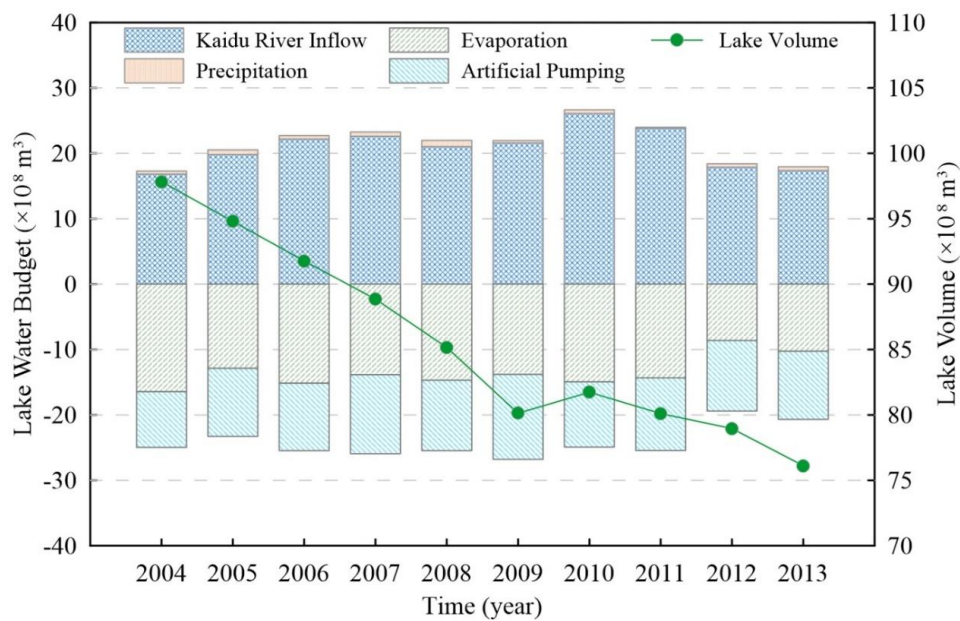


807

808 **Fig. 4.** The calibrated results of the transient model showing (a) observed vs. calibrated runoff  
809 at Yanqi station over time, (b) observed vs. calibrated runoff at Baolangsumu station  
810 over time; (c) observed vs. calibrated lake level over time; (d) comparison of observed  
811 and calibrated groundwater heads at all observation wells, and (e) observed vs.  
812 calibrated groundwater heads over time at three typical observation locations as labeled  
813 in Fig. 3.

814

815



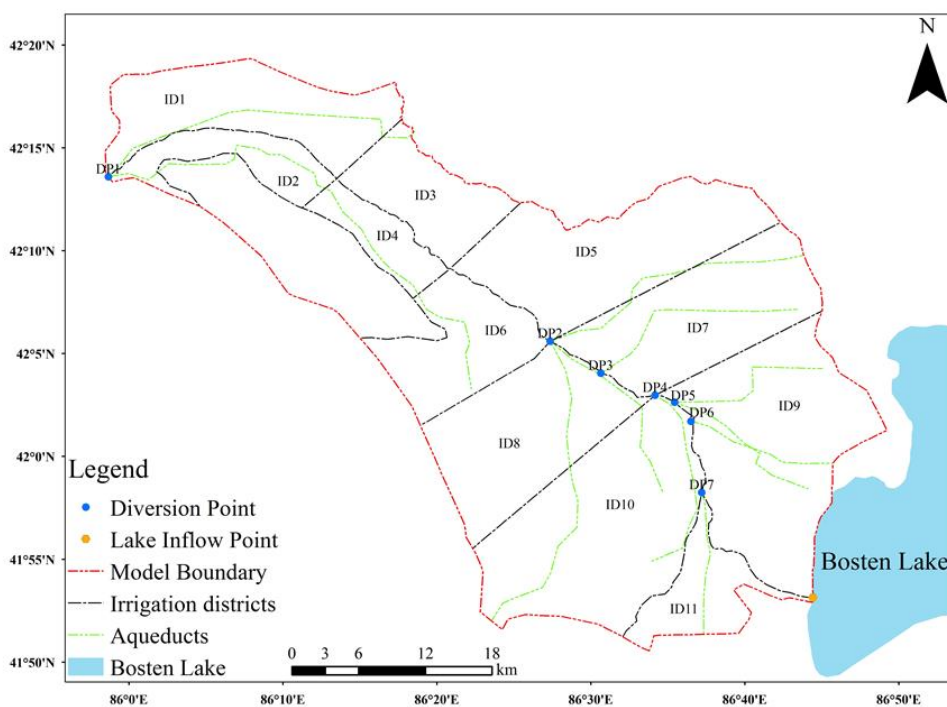
816

817 **Fig. 5.** The water balance terms of Bosten Lake and resulting lake volume in the simulation  
818 period.

819

820



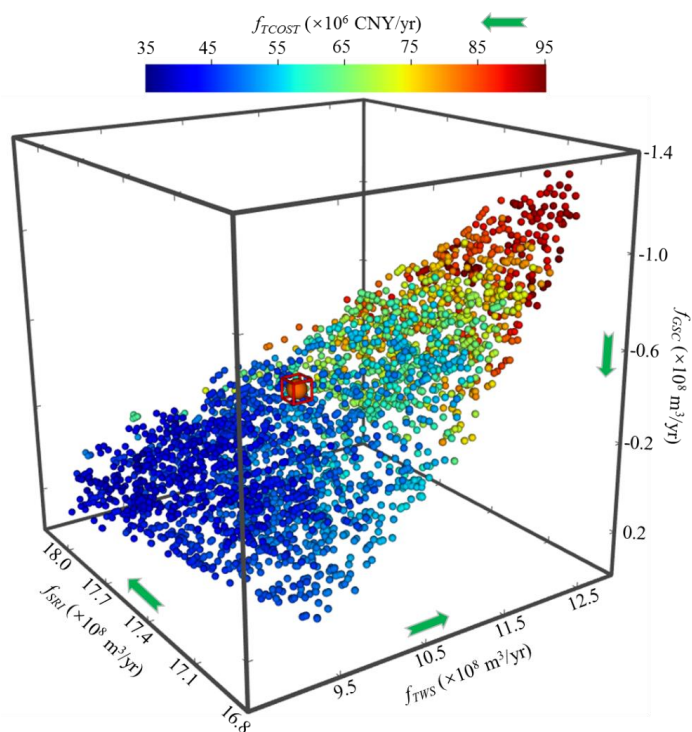


821

822 **Fig. 6.** The locations of surface water diversion points and subdomains of irrigation districts  
823 for groundwater abstraction.

824

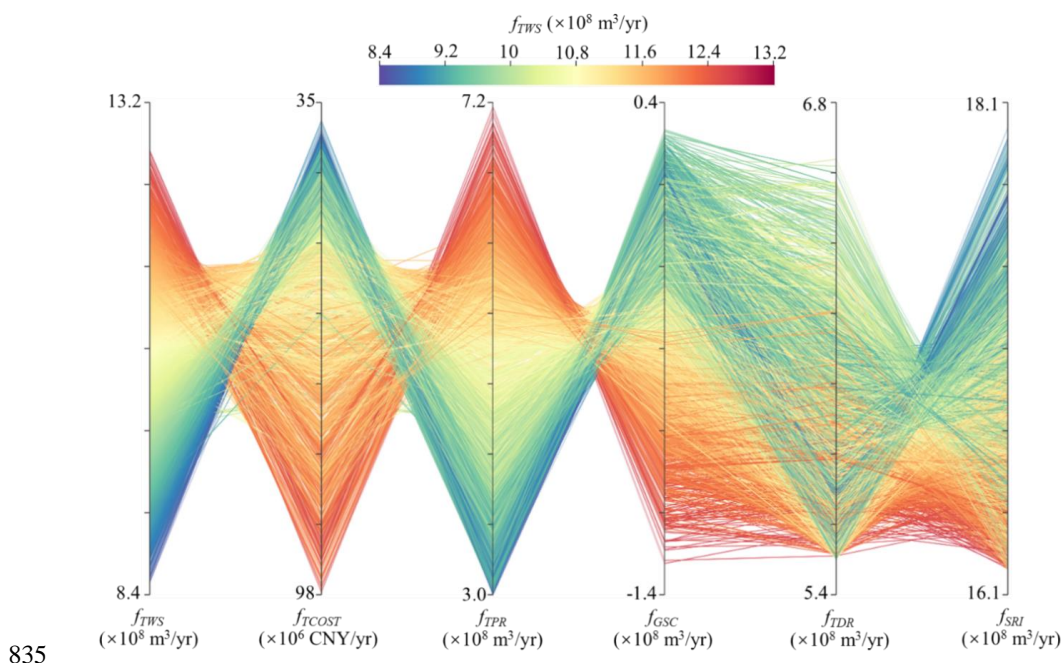
825



826

827 **Fig. 7.** The tradeoff surface to the integrated SW-GW management in Yanqi Basin. Each  
828 spheric symbol represents a water use scheme corresponding to specific objective  
829 values of the total water supply rate ( $f_{TWS}$ ), total cost of water delivery ( $f_{TCOST}$ ), surface  
830 runoff inflow to lake ( $f_{SRI}$ ) and groundwater storage change ( $f_{GSC}$ ).  $f_{TCOST}$  is symbolized  
831 in color to identify the objective value against others. The green arrow is the direction  
832 of better performance for each objective. The scheme before optimization is marked in  
833 a red square box.

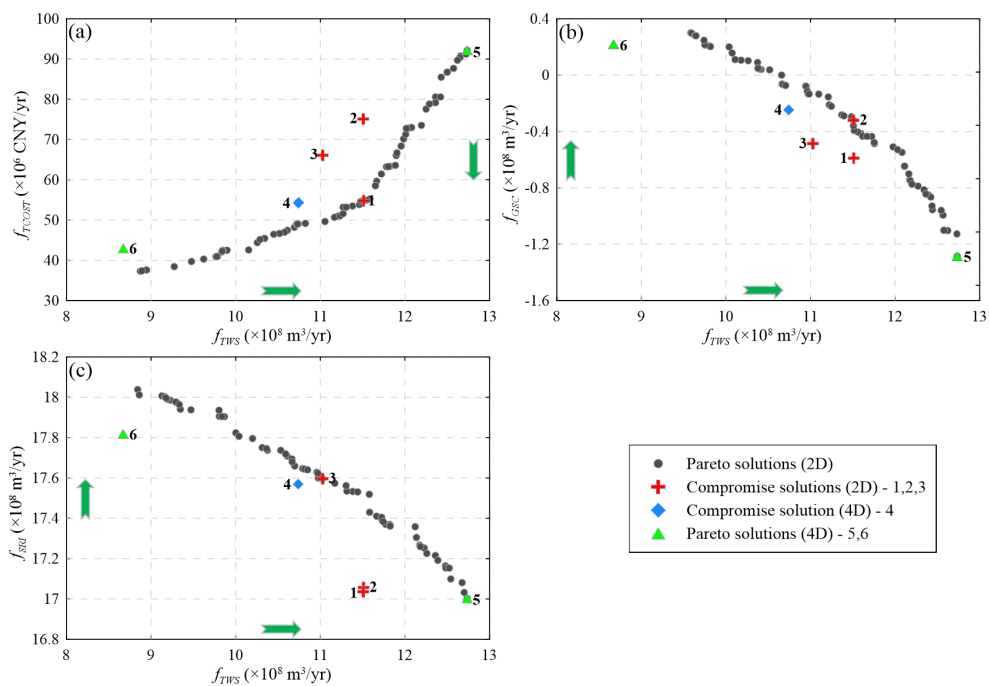
834



836 **Fig. 8.** The objective values (y-axis) are plotted over management objectives  $f_{TWS}$ ,  $f_{TCOST}$ ,  $f_{GSC}$ ,  
837  $f_{SRI}$ , total pumping rate  $f_{TPR}$  and total surface water diversion rate  $f_{TDR}$  (x-axis),  $f_{TWS}$  is  
838 represented in color. The preferred direction for each index is upward.

839

840

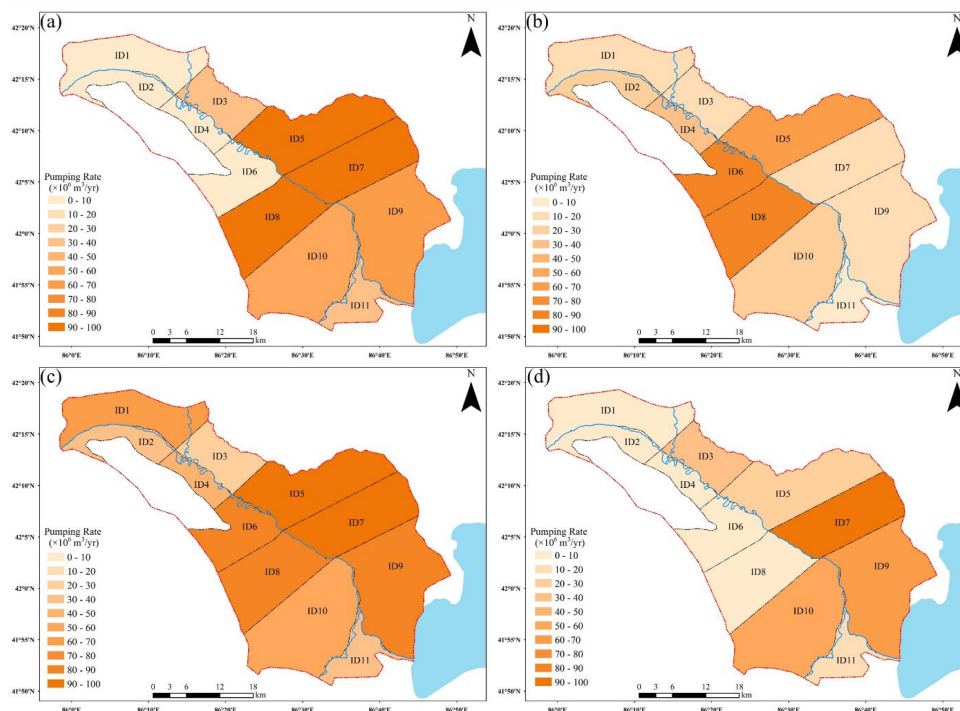


841

842 **Fig. 9.** Identification of six interesting solutions (Solutions 1-6) from the four-dimensional  
 843 approximate Pareto set and the green arrow is the preferred direction for each objective.

844

845

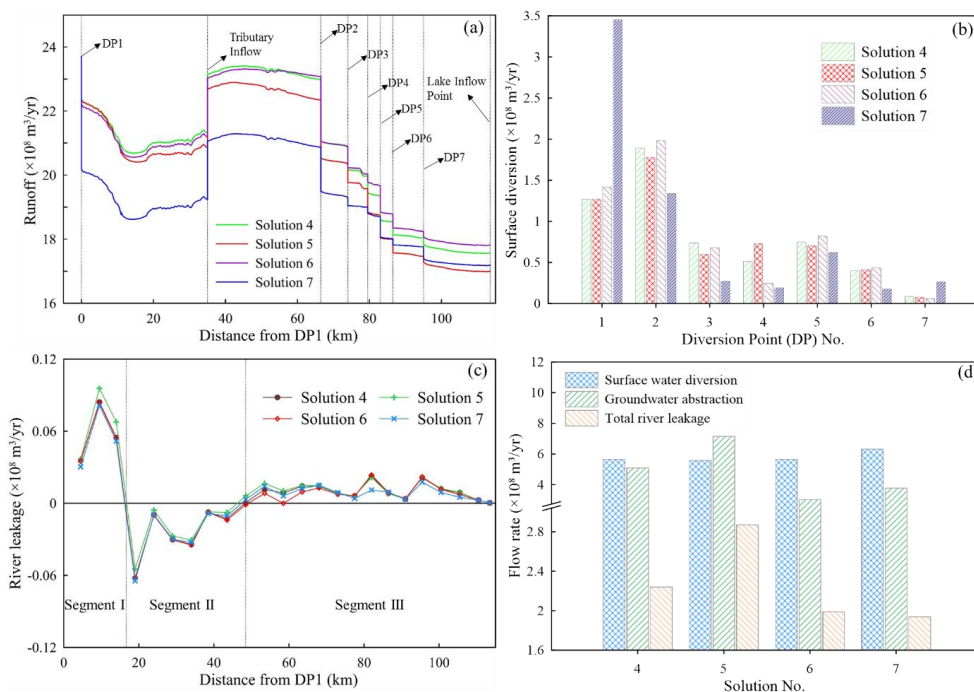


846

847 **Fig. 10.** The spatial distribution of the pumping rates in the 11 irrigation districts for the four  
848 selected schemes of (a) Solution 4, (b) Solution 7, (c) Solution 5, and (d) Solution 6,  
849 respectively.

850

851

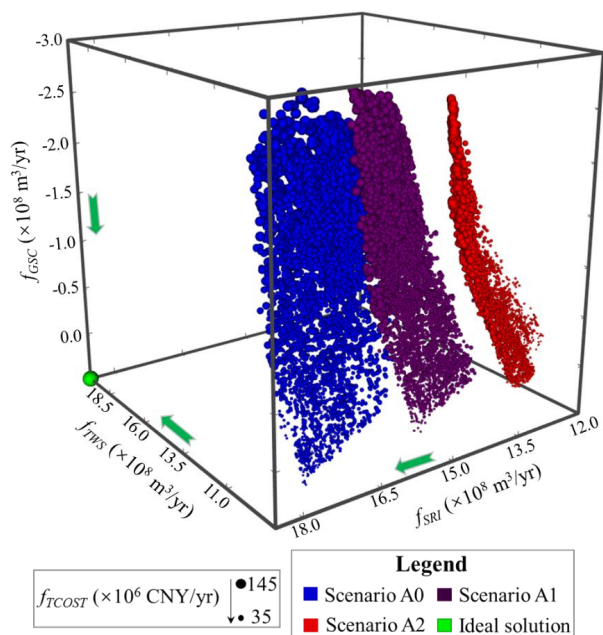


852

853 **Fig. 11.** Variation of surface runoff and river leakage along the stem stream of Kaidu River: (a)  
 854 the profile of river runoff; (b) the distribution of surface water diversion at the different  
 855 diversion points; (c) the profile of river leakage; (d) the components of total river  
 856 leakage, groundwater abstraction and surface water diversion for several typical  
 857 Solutions 4-7.

858

859

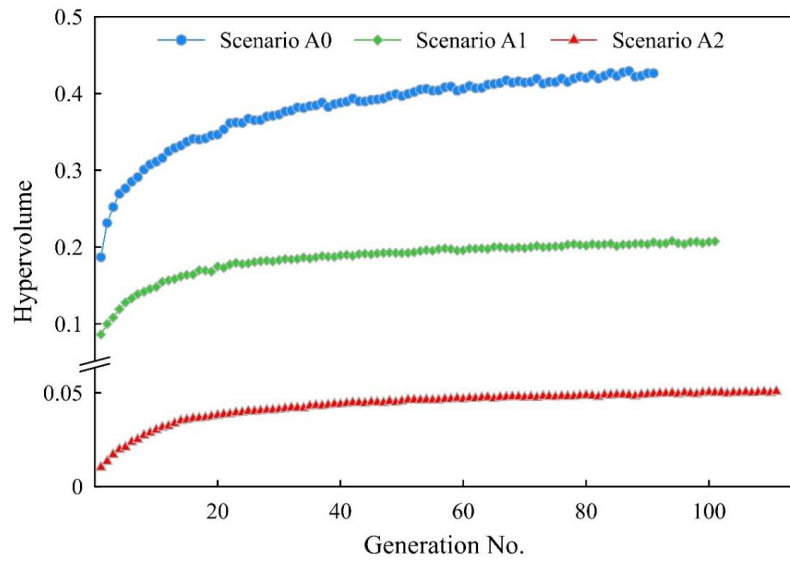


860

861 **Fig. 12.** The tradeoff solutions under Scenarios A0, A1 and A2, and the sphere size indicates  
862 the value of  $f_{COST}$ . The green arrow is the direction of better performance for each  
863 objective.

864

865

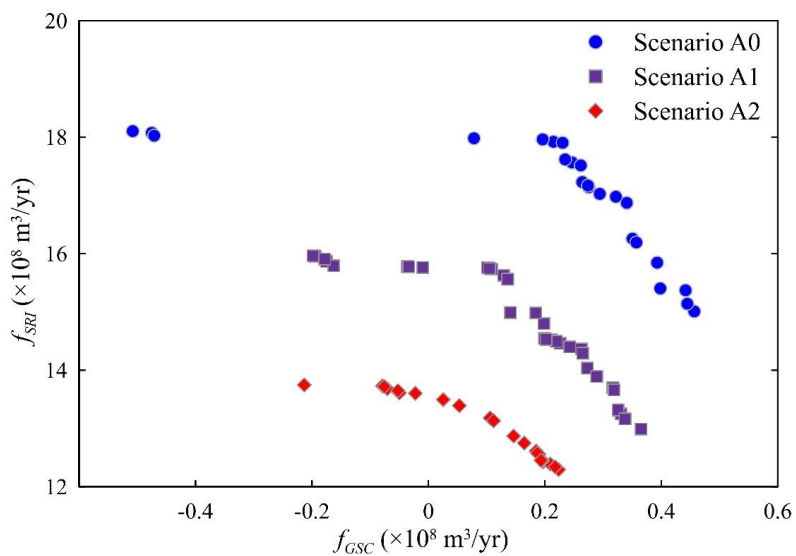


866

867 **Fig. 13.** Evolution of the hypervolume metric over the generation number for Scenarios A0, A1  
868 and A2.

869





870

871 **Fig. 14.** Non-dominated fronts of Scenarios A0, A1 and A2 between objectives of  $f_{GSC}$  vs.  $f_{SRI}$ .

872

873